Final Draft
of the original manuscript:

Dogan, B.; Ceyhan, U.; Petrovski, B.:
High Temperature Crack Initiation and Defect Assessment of P22 Steel Weldments using Time Dependent Failure Assessment Method
In: Engineering Fracture Mechanics (2006) Elsevier

DOI: 10.1016/j.engfracmech.2006.08.018

Paper to be published in the Elsevier Journal Eng. Fracture Mechanics

High Temperature Crack Initiation and Defect Assessment of P22 Steel Weldments using Time Dependent Failure Assessment Method

B.Dogan, U.Ceyhan and B.Petrovski

GKSS Research Centre, D-21502 Geesthacht, Germany

Abstract

High temperature deformation and crack resistance of low alloy ferritic grade P22 steel weldments applied in power plants are reported. The creep crack initiation (CCI) and creep crack growth (CCG) data were determined using compact type (C(T)) and C-Shape (CS(T)) fracture mechanics specimens at 550 °C. The deformation and crack growth behaviour of similar weldment zones and significance of CCI and CCG in defect assessment of components were addressed. The weldments with industrially relevant properties were produced in butt welded pipe joint from which test specimens are sampled. The studied material covers a spectrum of microstructures and ductility over the weldment zones to give representative for a welded component. The emphasis is placed on the measurement and particularly analysis of crack initiation for failure assessment in P22 steel weldments. The particular importance of construction of isochronous curves for time dependent failure assessment diagram (TDFAD) method is reported. It is aimed to contribute establishing guidelines for acceptable methodologies for testing, analysis and assessment of welded components using TDFAD for high temperature service.

Nomenclature

a	Crack length
a_o, a_f	Initial and final crack length measurements
Δa	Amount of crack growth
da/dt	Crack growth rate
A_1	Constant of Norton's creep law
B, B_n	Specimen thickness, net specimen thickness
CF	Constant Force
CCI, CCG	Creep Crack Initiation, Creep Crack Growth
C(T)	Compact Specimen in Tension
CS(T)	C-Shape Specimen in Tension
C^*	Steady state creep fracture mechanics parameter
$C^*(t)$	Experimentally determined value of C^* at test time, t
D_1	Constant of strain hardening law
E	Elastic modulus
E'	Effective elastic modulus for plane strain
$F_c(\theta)$	Shape function to determine creep zone size r_c
HAZ	Heat Affected Zone
J_T	Total value of crack tip parameter, J-integral
K	Stress intensity factor
K_r	Non-dimensional crack tip damage parameter of TDFAD
K^c_{mat}	Creep crack initiation toughness
L_r	Non-dimensional ligament damage parameter of TDFAD
L_r^{max}	Cut-off value of L_r
LLD	Load Line Displacement
m	Strain hardening exponent
n	Norton's creep law exponent
P	Applied load

PD	Potential Drop
r_c	Creep zone size at the crack tip
TDFAD	Time Dependent Failure Assessment Diagram
t	Time
t_i	Time for crack initiation (at Δa=0.2 mm and 0.5 mm)
t_I	Incubation time
W	Specimen width or half width
Δ_c	Creep component of load line displacement
$\dot{\Delta}_c$	Creep component of load line displacement rate
ε_{ref}	Reference Strain
η	Geometric factor to calculate C^*
σ	Stress
$\sigma_{0.2}$	0.2% proof stress; stress corresponding to 0.2% plastic strain
$\sigma^c_{0.2}$	0.2% inelastic strength; stress corresponding to 0.2% inelastic (plastic and creep) strain
σ_{ref}	Reference stress

1. INTRODUCTION

The recent progress made in defect assessment and lifing procedures contributes substantially to safety and reliability of plants [1,2]. Reviews on high temperature defect assessment procedures [3] and defect assessment at low to high temperature [4] emphasise the need for reliable data for design and in-service assessment. It is noted that design codes generally consider defect free structures, whereas assessment codes address flaws and their treatment. The British Standard document BS 7910 [5] contains some specialised data for creep crack growth assessment. There is no provision made in the ASME N-47 Code [6] for the assessment of short defects. The 'no initiation' criterion is based on factored laboratory endurance data where this constitutes failure of a specimen typically 8 mm in diameter. The problem of initiation and growth of defects from an assessment point of view has been presented step-by-step in 7 volumes in R5 [7]. The A16 procedure [8] for the initiation and growth of short cracks combines the RCC-MR concept of evaluating damage at a distance "d" from the crack tip which will lead to a finite size defect [9]. The approach considers the stress state at a distance d ahead of a notch-like defect, given by $\Delta K/(2\pi d)^{1/2}$ [10]. The 'microstructurally' short crack growth has been studied [9], where defects start, then become temporarily arrested at microstructural barriers such as grain boundaries.

The operational and plant assessment experience indicates that in the majority of cases where creep crack initiation and growth occurs, defects predominate in the vicinity of weldments. Therefore, high temperature failure by creep crack initiation (CCI) and creep crack growth (CCG) at structural joints imposes a limit on component service life of plants. The concepts used for time dependent fracture analysis of homogeneous bodies are commonly applied for CCG assessment of weldments. The crack growth rate is correlated with $C^*(t)$ in the extensive creep regime according to ASTM E1457 [11], the only available standard for creep crack growth testing of metallic materials, and with C_t parameter [12] in the small-scale creep to the extensive creep regimes. However, recent experimental data [13,14] and analytical evidence [15,16] has shown that $C^*(t)$ is not suitable for characterising creep crack growth behaviour in materials with low ductility in which the crack tip can advance at a rate comparable to the creep zone expansion rate. This directs attention to the crack tip parameters that correlate data in both creep ductile and creep brittle materials. Therefore, the stress intensity factor approach is revisited for materials that are in creep regime where the creep crack initiation toughness, K^c_{mat}, has been introduced [17]. Thus introduced materials creep toughness for crack initiation constitutes the fundamental concept for Time Dependent Failure Assessment Diagram (TDFAD) approach [18].

Furthermore, applicability of the crack tip parameters to crack growth of weldments with microstructural variations requires systematic studies to identify the relevant correlation parameter and its applicability in defect assessment. Linear elastic and elastic-plastic analysis of bi-material interface cracks show that the crack tip fields, and the size and shape of the plastic zones, are quite different for homogeneous and bi-material bodies. This indicates that the assumptions on which $C^*(t)$ is based are violated, thus supporting the approach taken for using TDFAD.

2. TIME DEPENDENT FAILURE

2.1 Creep Crack Initiation

The behaviour of specimens under creep loading conditions is described by load line displacement – time diagrams. On application of a steady (constant) force to a pre-cracked specimen the load point displacement increases with time. The creep zone ahead of the crack tip is defined as the region in which creep strain exceeds the elastic strain, the creep zone size increases with time according to,

$$r_c = K^2 (EBt)^{2/(n-1)} F_c(\theta)/2\pi \tag{1}$$

where $F_c(\theta)$ is a shape function as defined in [19] and n is the Norton's creep exponent. Microstructural damage occurs as a consequence of accumulation of creep strain. Initiation of creep crack requires attainment of critical local strain at the crack tip. The magnitude of time to initiate a creep crack, t_i, depends on the increment of crack extension, Δa_i, determined for the definition of crack initiation, x_c [20]. Therefore, the magnitude of t_i depends on the initiation criteria adopted, such as time to initiate a microcrack i.e. x_c=10 μm grain size, will be significantly less than that for a macrocrack, i.e. x_c=0.2 or 0.5 mm, the engineering definition of crack initiation as adopted in testing and assessment codes. Hence, determination of Δa_i, by using either the potential drop (PD) method or partial unloading compliance is of engineering importance as it directly affects the life of a structural component [21]. In engineering terms, detection of a crack using non-destructive testing (NDT) is required in service components that correspond to the adopted engineering macro crack initiation size. In component defect assessment, the data analysed to determine crack growth rate vs. crack tip parameter K or C^* usually give an initial "tail" with a decreasing growth rate prior to onset of steady-state growth rate. The tail represents the transition to steady state and depends on material properties and loading conditions. However, the data prior to steady state crack growth initiation, defined at crack extension, Δa, of 0.2 or 0.5 mm reflect the stress redistribution and development of damage. Therefore, it needs to be recorded and analysed as it may cover a large portion of component life in service.

2.2. Estimation of Crack Initiation Time

The incubation period is the time required for sufficient damage accumulation at the crack tip leading to onset of crack growth. The incubation period can be estimated from the equations where data are not available for the material used for the component. The incubation time defined is calculated using [22]

$$t_I = 0.0025 \left[\frac{\sigma_{ref}\, t_{R(ref)}}{\left(K_a^p\right)^2} \right]^{0.85} \tag{2}$$

The incubation time for the component in secondary creep stage can be obtained from the following equations when incubation time data are available from test specimens

$$\left(\frac{t_{Icomp}}{t_{Ispec}} \right) = \left(\frac{C^*_{spec}}{C^*_{comp}} \right)^{\frac{n}{n+1}} \tag{3}$$

where subscripts comp. refers to the component and spec. refers to the specimen.

2.3. Time Dependent Failure Assessment Diagram (TDFAD)

Failure Assessment Diagram (FAD) methods, such as in R6 [23], have been developed to assess defect containing components. The FAD method has been extended to the creep regime, named as TDFAD [18]. The advantages of using a TDFAD are: a) detailed calculations of crack tip parameters such as C_P are not needed, b) it is not necessary to establish the fracture regime in advance and c) the TDFAD can indicate whether failure is controlled by crack growth in the small-scale or widespread creep regime or by creep rupture. However, note that the TDFAD is developed based on the experience on austenitic steels where the material behaviour may differ from that of ferritic materials. This issue will be addressed in the present paper as follows.

2.4. Construction of TDFAD

The TDFAD is a two-parameter failure assessment diagram, which takes both ligament failure and crack propagation into account [24]. In other words, the TDFAD combines fracture mechanics which describes crack tip failure and damage mechanics that describes ligament failure. After the construction of TDFADs for the test times of interest, the failure initiation time for a specimen/component is estimated by intersecting the line constructed joining the points obtained for the TDFAD parameters. The TDFAD is based on the Option 2 FAD specified in R6 [23] with a failure assessment curve correlating two parameters K_r and L_r.

In the TDFAD, the parameters K_r and L_r are defined as:

$$K_r = K / K^c_{mat}, \quad \text{and} \quad L_r = \sigma_{ref} / \sigma^c_{0.2} \tag{4}$$

where, K is the stress intensity factor, K^c_{mat} is the material's creep crack initiation toughness corresponding to a given crack extension at a given time and $\sigma^c_{0.2}$ is the stress corresponding to 0.2% inelastic (creep and plastic) strain from an isochronous stress–strain curve at a particular time and temperature. K^c_{mat} is the fundamental concept for TDFAD, at a particular time and crack extension. The details of the TDFAD assessment approach are given in [18].

The application of the TDFAD can be summarised in 5 steps [24]:

1) Define the maximum tolerable crack extension Δa for the creep crack initiation (CCI) (i.e. Δa=0.2 mm or 0.5 mm).
2) Construct isochronous curves using uniaxial creep data (Fig.1).
3) Obtain $\sigma^c_{0.2}$, σ_r from isochronous curves obtained for each time of interest.
4) Construct the TDFAD for each time of interest (i.e. t = 100h – 50,000 h) using the related formulae:

$$K_r = \left[\frac{E\varepsilon_{ref}}{L_r \sigma^c_{0.2}} + \frac{L_r^3 \sigma^c_{0.2}}{2E\varepsilon_{ref}} \right]^{-1/2} \qquad \text{for} \qquad L_r \le L_r^{max} \tag{5.a}$$

$$K_r = 0 \qquad \text{for} \qquad L_r > L_r^{max} \tag{5.b}$$

In equation (5), E is Young's modulus and ε_{ref} is the total strain from the average isochronous stress-strain curve at the reference stress, $\sigma_{ref} = L_r \sigma^c_{0.2}$, for the appropriate time and temperature. $\sigma^c_{0.2}$ is obtained from the isochronous stress-strain curve for the time of interest. Thus, equation (5) enables the TDFAD to be plotted with K_r as a function of L_r. The cut-off, L_r^{max}, is defined as

$$L_r^{max} = \sigma_R / \sigma^c_{0.2} \tag{6}$$

where σ_R is the rupture stress from creep tests for the time and temperature of interest.

5) Determine values of material creep crack initiation toughness, K^c_{mat}, for each time of interest for the specified maximum tolerable crack extension distance, Δa (i.e. 0.2 or 0.5 mm).

6) Calculate values of TDFAD parameters, L_r and K_r, for the time for which the occurrence of CCI is needed to be predicted. If the point obtained lies within the safer zone of TDFAD, the crack is not initiated.

The application procedure of the TDFAD is illustrated schematically in Figure 2. The first step of the construction and application of the TDFAD is to decide on the engineering definition of crack extension Δa, for which the crack is adopted to be started (Δa = 0.2 mm or 0.5 mm) [25].

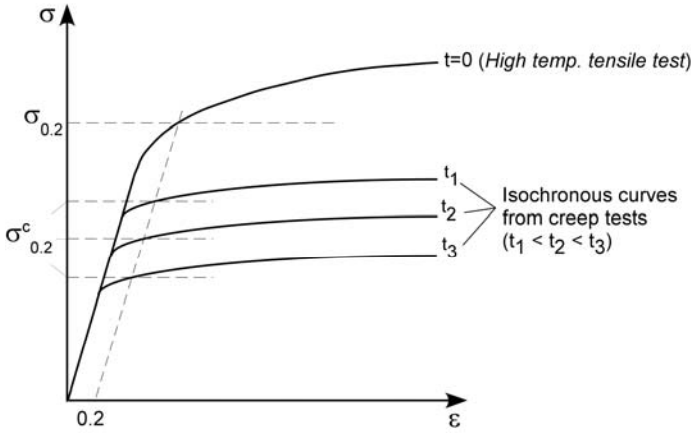

Figure 1 – Schematic isochronous stress-strain curves indicating the definition of $\sigma^c_{0.2}$

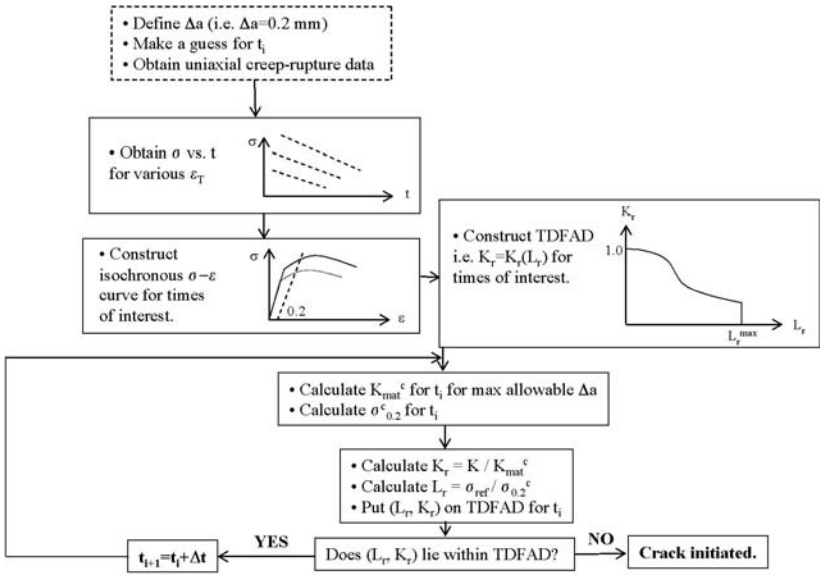

Figure 2 – Flow diagram of the application of TDFAD

3. EXPERIMENTAL DATA

3.1. Mechanical and Creep Properties

The mechanical and creep properties of weld materials were determined at 550 °C as given in Table 1. The yield strength data at test temperature show a decrease in the WM and particularly in the HAZ. This indicates undermatched welds in terms of strength values.

Table 1 – P22 weld materials data determined in tensile and creep tests at 550 °C

Material	$R_{p0.2}$(MPa)	R_m(MPa)	E(GPa)	D_1	m	A_1	n
P22 BM-550 ^oC	350	397	157	0.0024	16.91	$2.80x10^{-43}$	17.80
P22 WM-550 ^oC	327	369	136	0.0016	19.17	$7.64x10^{-21}$	7.40
P22 SIM. HAZ-550 ^oC Type IV	241	345	108.3	0.0017	8.51	$1.09x10^{-22}$	8.48
P22 SIM. HAZ-550 ^oC Centre	320	381	144.8	0.0016	12.20	$9.55x10^{-17}$	5.99

Note: The constants relate to stress-strain (D_1, m) and steady-state creep (A_1, n) behaviour.

The yield strength of WM and particularly in the HAZ-Type IV section is lower than that of the BM. Therefore, the welds are undermatched in terms of yield strength. However, note that the creep resistance of a material rather than the yield strength determine the crack initiation and growth behaviour under creep conditions. Therefore, creep strength values of the materials are taken for comparison with the terminology of creep strong or creep weak to emphasise the different deformation processes at high temperature where the mismatch concept is used, and low temperature behaviour.

3.2. Creep Crack Initiation and Growth Tests

Constant force tests were carried out for obtaining CCI and CCG data. The force, potential drop (PD) and load line displacement (LLD) data are logged all the way to full load starting from pre-load for the subsequent analysis of the data for crack size and crack tip parameters C^* and K determination. In addition, the force/displacement measurements give the specimen's elastic compliance for the initial and final crack lengths.

3.2.1. Crack Size Determination

The direct current potential drop (DCPD) method was applied to monitor the crack initiation and growth during testing. The crack size was determined from PD data using Johnson's formula given for the C(T) geometry [11]. Correct use of PD data is particularly important to determine the CCI due to possible variation of the PD-time records [21].

The scatter in crack size using the PD method is increased by the crack tunnelling as observed on fracture surfaces as seen in Figure 3. An accurate measure of the initial, a_o, and final, a_f, crack front and crack size were made when the specimen was broken open outside the furnace after testing. The irregularities of crack growth path are considered [5] for reliable crack length determined on the fracture surface.

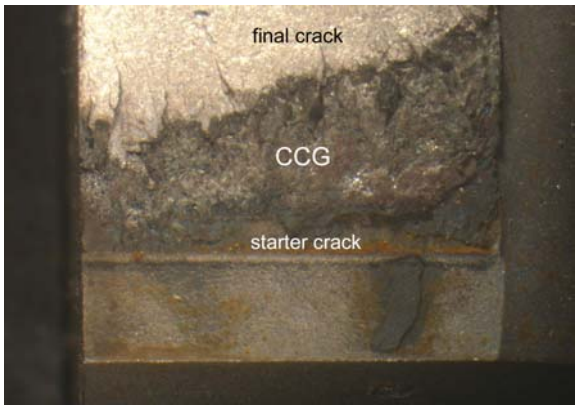

Figure 3 – Fracture surface of a tested CS(T) specimen of BW P22 with starter crack in WM. Sectioned specimen half

3.3. Data Assessment and Crack Initiation and Growth Correlations

The complete experimental data set was assessed and the CCG rate materials was correlated with the crack tip parameter C^* in Figure 4. A good correlation is seen, particularly at steady state crack growth rates, especially for P22 WM, following the crack initiation in the transition range (Fig. 4(a)). The scatter is high in tails and in the later stage of crack growth particularly for P22 HAZ (Fig. 4(b)). These results call for detailed study of CCI and contribution of plasticity in the final stage of crack growth.

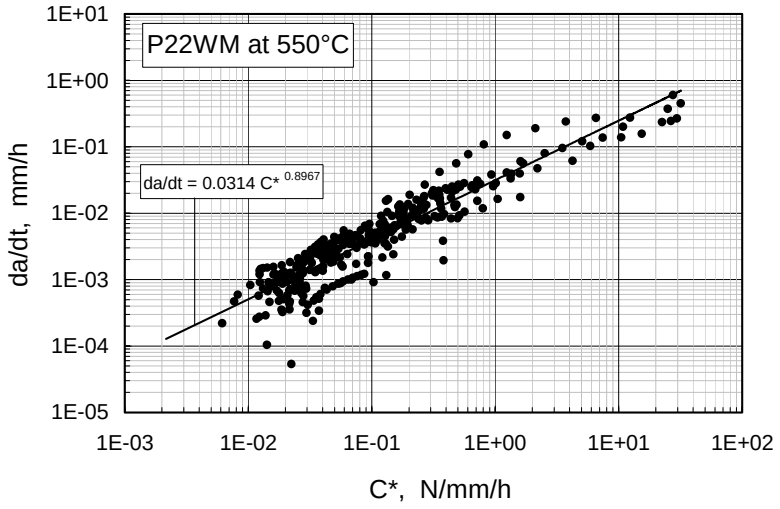

(a)

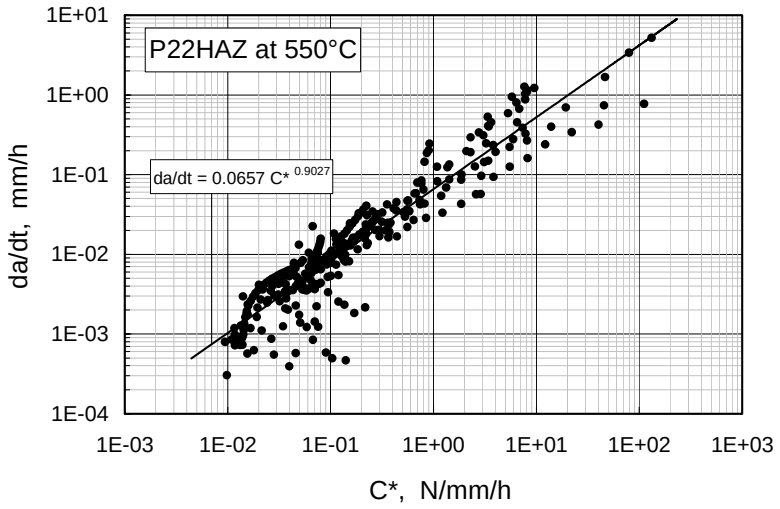

(b)

Figure 4 – High temperature creep crack growth behaviour of (a) P22 weld metal (WM) and (b) P22 heat affected zone (HAZ) at 550 °C.

3.3.1. Correlation of Crack Initiation

The experimental data obtained on P22 steel weldments including weldment zones of base metal (BM), heat affected zone (HAZ) and weld metal (WM) are shown in Figures 5-7. The data are correlated with K where crack initiation is defined at Δa of 0.2 and 0.5 mm of crack extension as depicted in Figures 5 and 6, respectively. The data from HAZ show a rapid decrease in crack initiation resistance at longer test times compared with BM and WM data as seen in best fit lines. Time to crack initiation defined at Δa=0.2 mm is correlated with C^* in Fig.7. A good correlation directs attention to

use of C^* data for CCI assessment. However, note there is no anomaly in correlation of crack initiation resistance of materials from different zones of the weldment.

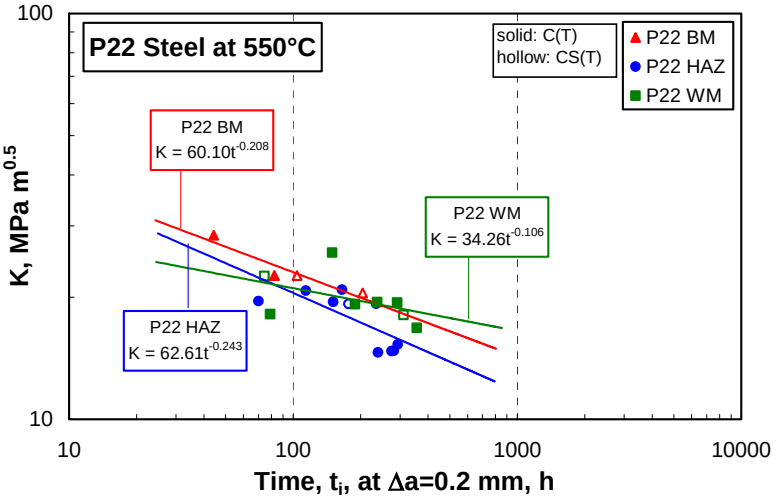

Figure 5 – Crack initiation resistance K of P22 similar weldment zones (BM, HAZ, WM) at 550 °C as a function of time to crack extension (Δa) of 0.2 mm.

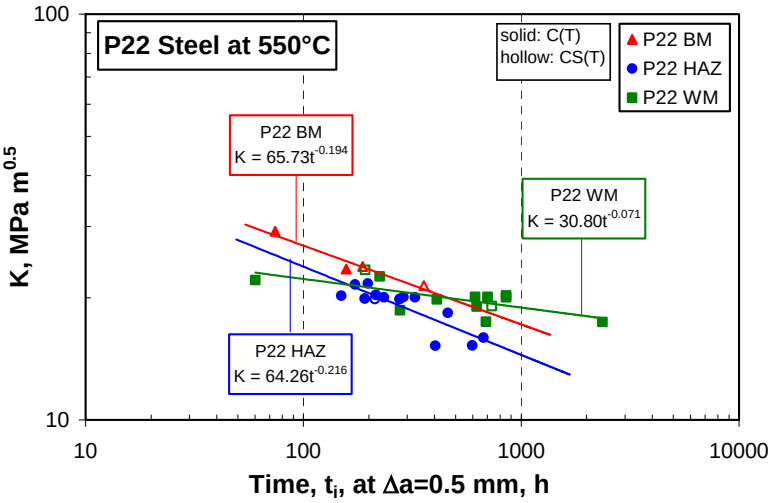

Figure 6 – Crack initiation resistance K of P22 similar weldment zones (BM, HAZ, WM) at 550 °C as a function of time to crack extension (Δa) of 0.5 mm.

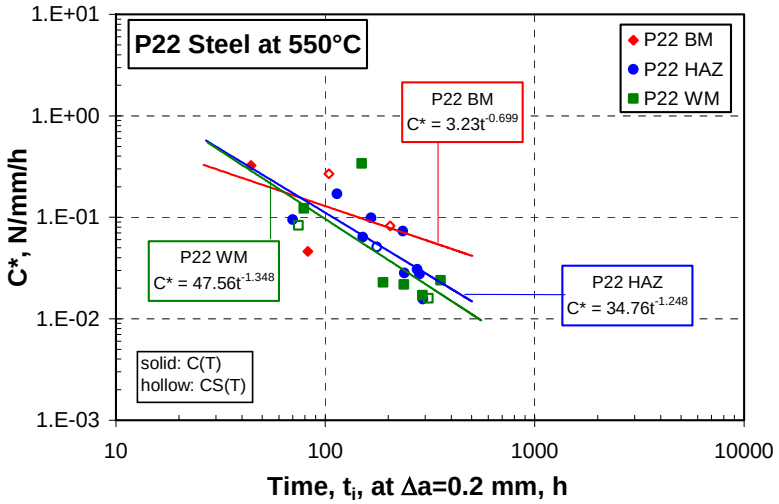

Figure 7 – Creep crack initiation resistance C^* of P22 similar weldments zones (BM, HAZ, WM) at 550 °C as a function time for crack extension (Δa) of 0.2 mm.

The micromechanical approach taken by Pique et al. [26] relies on C^* to predict creep crack initiation time that involves the use of C^* vs. time diagrams, established for a material at temperature and crack initiation criterion. A typical crack size for initiation is taken as 50 µm, based on direct experimental observation. This approach is also based on the argument that the use of C^* to describe creep crack behaviour is only rigorously valid for stationary cracks. Therefore, it is employed only to correlate creep crack initiation times. Figure 7 shows C^* vs. crack initiation time data that sheds some light on the crack initiation defined in terms of micro and macro crack size.

The scatter increases in the C^* correlation that directs attention to the choice of crack tip parameter for crack initiation studies. Better correlation is seen at larger crack size times of Δa=0.2 mm as in engineering crack initiation definition.

3.4.Time Dependent Failure Assessment Diagram (TDFAD) Approach

A central feature of the TDFAD approach is the definition of an appropriate creep crack initiation toughness, K^c_{mat}. When used in conjunction with the failure assessment diagram, it ensures that crack growth in the assessment period is less than a value Δa. Creep crack initiation toughness values may be estimated indirectly from conventional creep crack incubation and growth data or evaluated directly from experimental load versus displacement information [17]:

$$K^c_{mat} = \left[K^2 + \frac{n}{n+1} \frac{E\,P\,\Delta_c}{B_n (W-a)} \eta \right]^{1/2} \tag{7}$$

where η is the geometric factor used for determining C^*, K is the stress intensity factor of the specimen and Δ_c is the experimental load line displacement due to creep at the time for which the crack extension is equal to Δa. Variation of K^c_{mat} with time for various weldment zones are plotted in Figures 8 and 9 for Δa=0.2 mm and 0.5 mm, respectively. Note that the scatter in the correlated data is higher than that of K and C^* correlations in Figures 5-7. However, the comparison of slopes of different weldment zones points out that there is a similarity between K^c_{mat} and C^* correlations. However, note higher slope of best fit data from BM than the two other weldment zones seen in K^c_{mat} correlation in Fig. 9, indicating decreased creep crack initiation toughness resistance at long times. These observations direct attention to the method used in TDFAD approach, as the TDFAD has been used successfully for austenitic steels. Use of the TDFAD in ferritic steels as in the present study, will

spread the applicability of the approach to a wider range of high temperature materials. This requires more data and further insight into the approach for its applicability to ferritic materials.

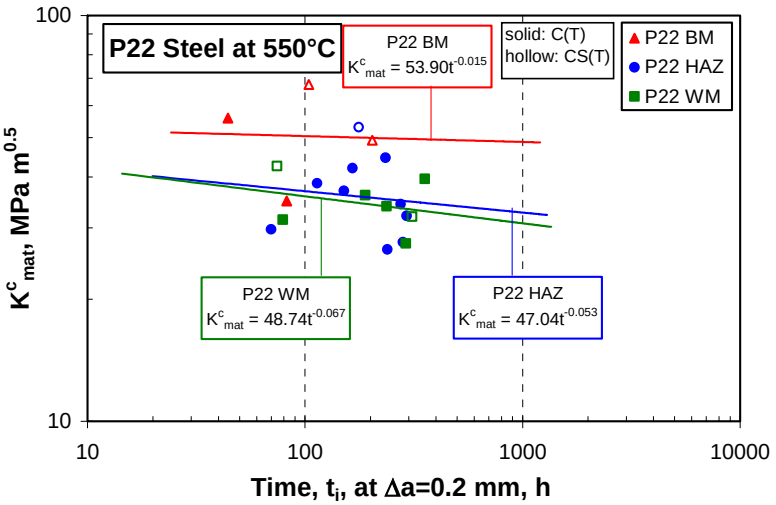

Figure 8 – Creep crack initiation toughness K^c_{mat} of P22 similar weldment zones (BM, HAZ, WM) at 550 °C as a function of time to crack extension (Δa) of 0.2mm.

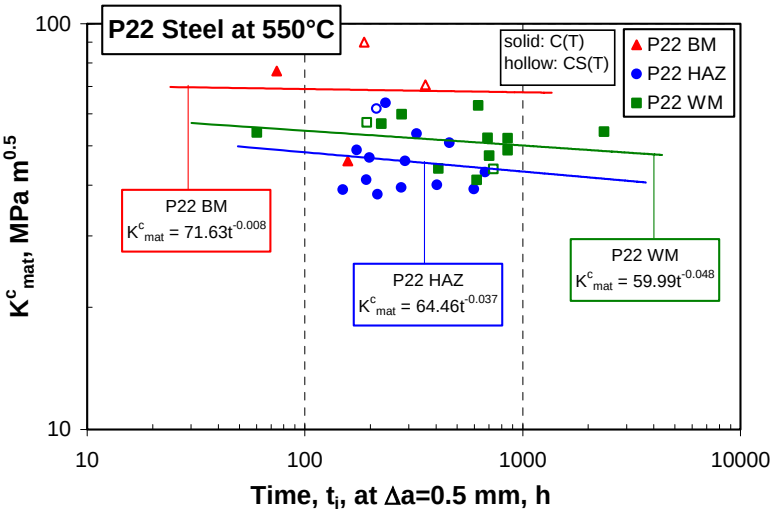

Figure 9 – Creep crack initiation toughness K^c_{mat} of P22 similar weldment zones (BM, HAZ, WM) at 550 °C as a function of time to crack extension (Δa) of 0.5mm.

The TDFAD method is applied to P22 similar weldment data shown in Figures 10-15. The TDFADs are determined for various times of 100 to 100,000 h. K_r and L_r values are calculated for crack initiation times defined at crack growth of Δa=0.2 mm and 0.5 mm for experimental CCG specimens. The data are plotted in Figures 10, 12 and 14 for BM, WM and HAZ, respectively. Note that in calculating K^c_{mat} only the creep component of the total strain energy is used. The crack initiation resistance of specimens from different microstructural zones of weldments show a dependence on loading condition as seen for C(T) and CS(T) specimens in Figs. 10, 12 and 14

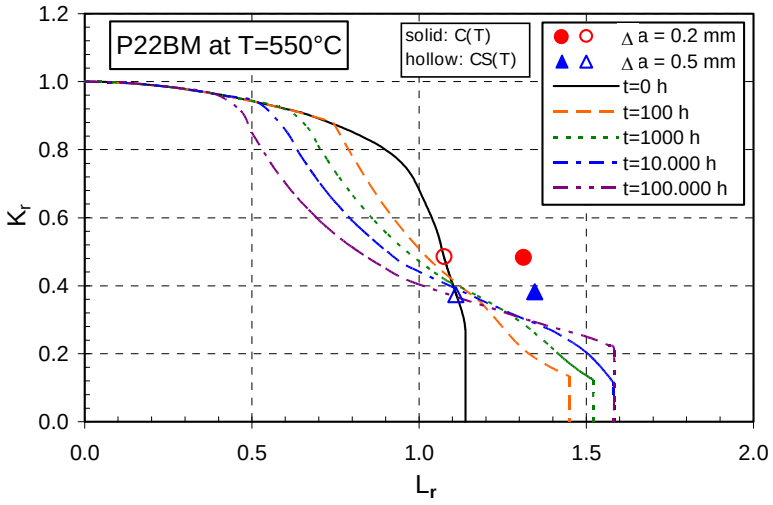

Figure 10 – TDFAD of P22 BM at 550 °C with experimental data for crack growth Δa=0.2 mm and 0.5 mm

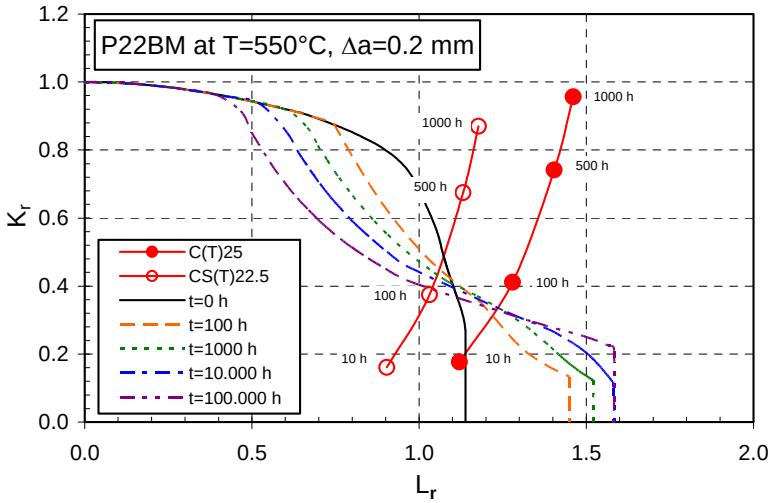

(a)

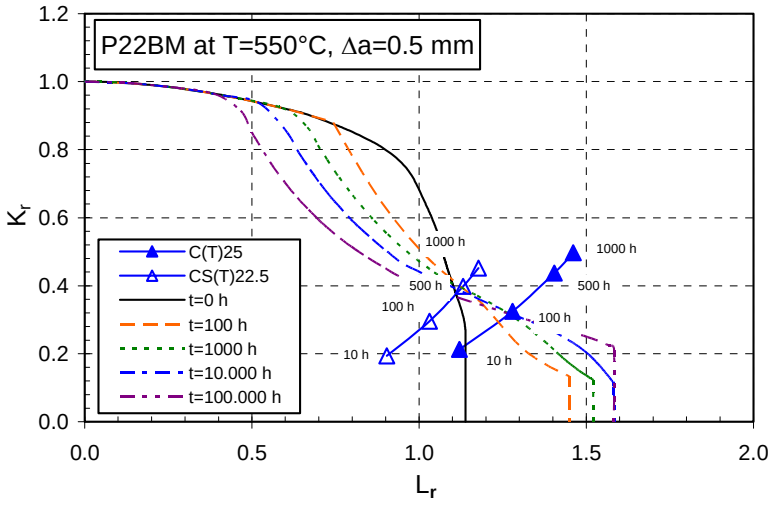

(b)

Figure 11 – TDFADs of P22 BM at 550 °C with predicted initiation times of 10, 100, 500 and 1000 hours for K^{c}_{mat} at Δa=0.2 mm (a) and 0.5 mm (b). C(T) specimen solid symbols, and CS(T) specimen hollow symbols

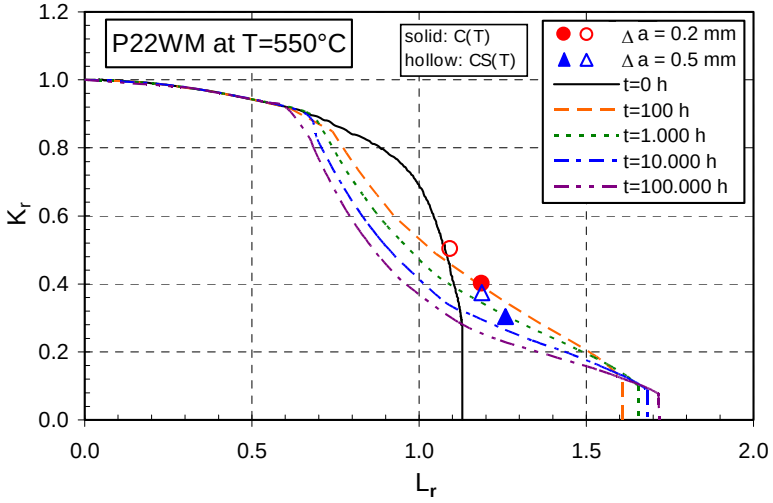

Figure 12. – TDFAD of P22 WM at 550 °C with experimental data for crack growth Δa=0.2 mm and 0.5

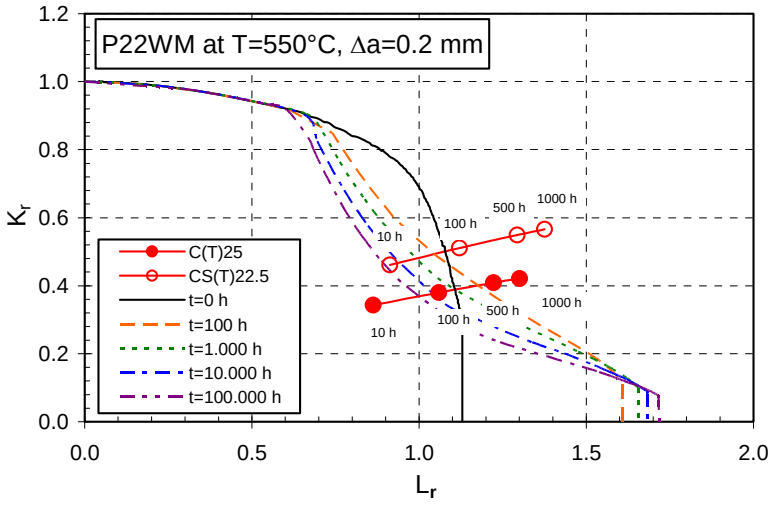

(a)

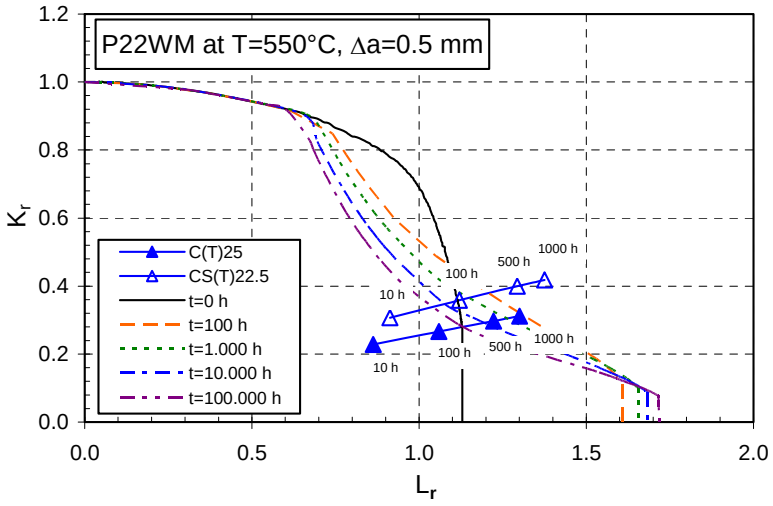

(b)

Figure 13 – TDFADs of P22 WM at 550 °C with predicted initiation times of 10, 100, 500 and 1000 hours for K^{c}_{mat} at Δa=0.2 mm (a) and 0.5 mm (b). C(T) specimen solid symbols, and CS(T) specimen hollow symbols

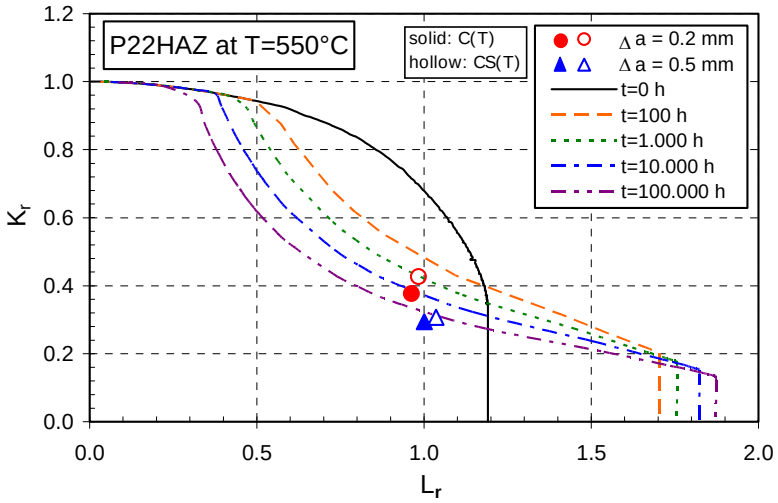

Figure 14 - TDFAD of P22 HAZ at 550 °C with experimental data for crack growth Δa=0.2 mm and 0.5 mm

Furthermore, the experimental data from C(T) and CS(T) specimens are compared with predictions. The predicted initiation times of 10, 100, 500 and 1000 h for K^{c}_{mat} values determined at Δa=0.2 and 0.5 mm are shown in Figures 11, 13 and 15 for BM, WM and HAZ, respectively. Thus, obtained initiation curves serve for prediction of time required for a specific amount (i.e. 0.2 or 0.5 mm) of crack extension. The different prediction lines indicate the difference in deformation behaviour of the respective material zones of BM, HAZ and WM.

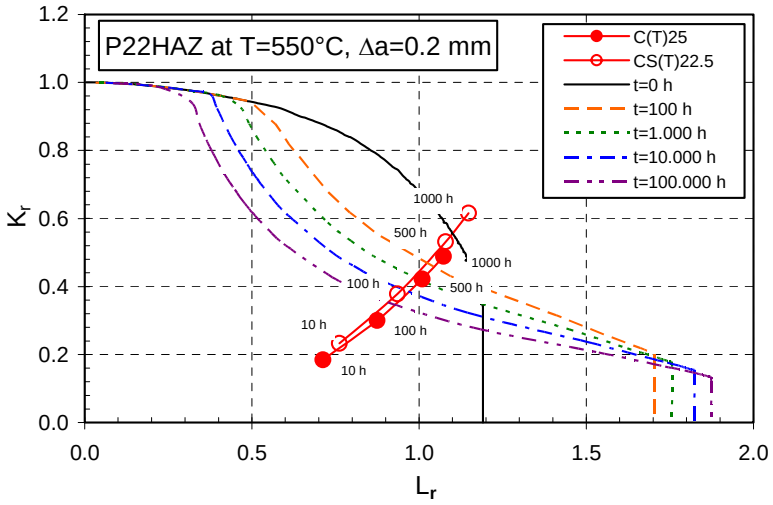

(a)

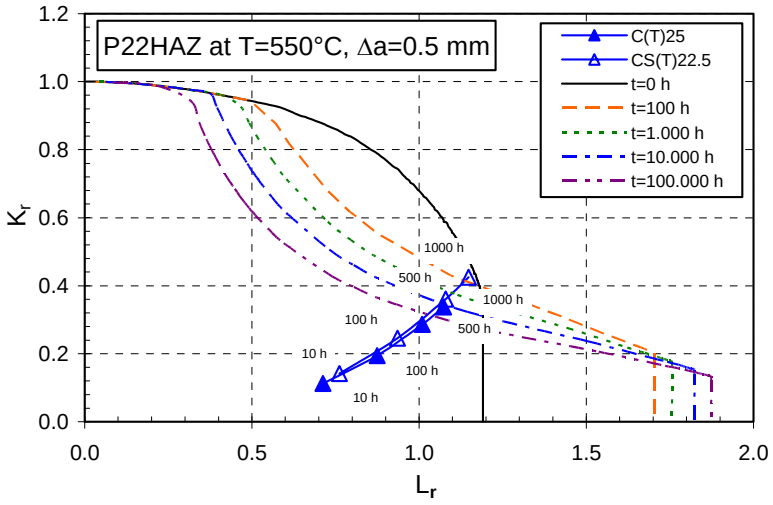

(b)

Figure 15 – TDFADs of P22 HAZ at 550 °C with predicted initiation times of 10, 100, 500 and 1000 hours for K^c_{mat} at Δa=0.2 mm (a) and 0.5 mm (b). C(T) specimen solid symbols, and CS(T) specimen hollow symbols

4. DISSCUSSION

The engineering definition of creep crack initiation is the time required for an amount of crack extension (Δa), i.e. Δa = 0.2 or 0.5 mm, similar to the definition of material's yield strength at 0.2 percent strain.

The experimental data also show a shift in high K data to longer times for crack initiation at Δa=0.5 mm compared to those for Δa=0.2 mm. However, the crack initiation time at lower K data obtained from HAZ and BM specimens are relatively unaffected with respect to the initiation crack size criterion. Similar crack initiation times are seen in Figs. 5-6 for HAZ. This indicates the higher creep crack initiation resistance of WM. In other words, it emphasises the importance of applicability of the crack tip parameters, K or C^*, for defect assessment under service loading conditions. This approach also forms the basis for low to high temperature defect assessment concept [4], where the transition from K to C^* correlation is studied.

The approximate initiation times are obtained for defined crack extensions of 0.2 or 0.5 mm. The value of K^c_{mat} on which the TDFAD is based, is obtained from the area under the load–displacement curve up to crack initiation defining the total J-integral value, J_T. K^c_{mat} is calculated from $K^c_{mat} = \sqrt{E' J_T}$. A polynomial equation is fit to the load–displacement data during load-up of the CCG test. Alternatively, in scarcity of test data in the initial parts of the test, only the creep component of J can be used to calculate K^c_{mat}. This allows neglecting elastic and/or plastic components since the creep component of total displacement is the major portion till crack initiation. Values of K^c_{mat} for crack extension, Δa, of 0.2 or 0.5 mm have been determined (Fig. 8, 9). Hence, the TDFAD is used to predict initiation time of the tests on standard C(T) and CS(T) specimens. The experimental initiation times of the tests have been compared to the predicted values in Figs. 9, 10. The predicted initiation time is sensitive to the variability in the creep crack initiation toughness and the determination of isochronous stress-strain data. Therefore, prediction of K^c_{mat} requires reasonable amount of experimental data which is a key issue in using the TDFAD.

Failure assessment diagrams are constructed for various times up to 100,000 h which provide a refined initiation time estimate. Time dependence of the TDFAD for certain loading conditions may not be

significant. Estimate of initiation times may be made from a TDFAD curve evaluated at a single time, e.g. 1000 h. Thus, the TDFAD is used to predict if a crack will extend a distance Δa in a given time (Figs. 10,12 and 14) or the time required for a specified amount of crack extension (Figs. 11, 13 and 15) for microstructural zones of BM, WM and HAZ. The experimental data presented in Figs. 10, 12 and 14 show optimistic estimate of TDFAD for all microstructural zones, particularly for HAZ, which is contradictory with the conservative diagrams obtained for different weldments zones of P91 [27]. The predicted crack initiation times show a dependency of material zones with larger times for HAZ (Fig 15). Crack initiation at Δa=0.2 mm is expected in a short time interval, whereas crack extension to 0.5 mm requires relatively higher times.

In order to predict the crack initiation time for the specimen, a locus of data points at times of 10, 100, 500 and 1000 h has been constructed on the TDFAD. Note that predicted loci depend also on plane stress and plane strain limit load solutions as discussed in detail in [28]. The lowest L_r or K_r locus corresponds to the lowest time of 10 hrs, where its value increases with time. Note that for a certain prediction line (Figs. 11, 13 or 15), the K_r value and the L_r value do not vary with the same rate with increasing time. This is due to the difference between rates of reduction in $\sigma^c_{0.2}$ and K^c_{mat} with time. Differences between different weldment zones are also noted. This indicates as well, the variation in high temperature fracture behaviour of different weldments zones. Thus the determined loci points enable prediction of crack initiation for a specimen for 0.2 mm and 0.5 mm crack with respect to the TDFAD for times 100 to 100,000 h (Figs.11, 13 and 15).

The shapes of the constructed TDFADs vary for BM, WM and HAZ reflecting the variation in creep deformation behaviour of different weldment zones. This indicates that the TDFAD approach captures different deformation behaviour in different zones that increases confidence in its use in defect assessment of welded components.

5. CONCLUSIONS

The significance of crack initiation for defect assessment of welded materials at high temperature is addressed. The findings are directly relevant to engineering structures where damage and CCI occurs predominantly in functionally graded material zones of weldments.

Creep crack initiation and crack growth have been studied using C(T) and CS(T) specimens of P22 similar welds at 550°C. Creep crack growth rate data are correlated with C^* which showed tails with higher scatter in correlated data. Therefore, the crack initiation has been studied experimentally and compared with predicted data. The crack initiation was defined at crack extension, Δa, of 0.2 and 0.5 mm. Times to crack extension Δa = 0.2 and 0.5 mm were plotted as a function of K, K^c_{mat} and C^*. The TDFAD approach has been chosen to investigate further the failure conditions and crack initiation. Values of K^c_{mat} were obtained for two crack initiation sizes, Δa of 0.2and 0.5 mm, that necessitate accurate data from the loading–up part of CCG tests. Such data are obtained from initial part of high temperature fracture mechanics test data where load is increased incrementally to the test load value in constant force tests. TDFADs have been produced for times varying from 100 h to 100,000 h. The shape and sequence of curves depend on the microstructural constituents (BM, WM, HAZ) of weldments. Initiation times have been predicted for specimens using the TDFAD approach that varied between 10 to 1000 h. Work is underway for prediction of creep crack initiation using German two criteria diagram approach, which is essentially similar to the presented TDFAD, however, constructed initially for ferritic homogeneous materials.

ACKNOWLEDGEMENTS

The authors would like to thank Drs. R. A. Ainsworth and D. W. Dean for providing material and fruitful discussions on TDFAD method.

REFERENCES

[1] Steen W. M. and Shannon, G. J., Proc. Int. Conf. Trends in Welding Research, Eds., J. M. Vitek et al., ASM International, 1998, p.423.

[2] Nikbin, K. M., Proc.Int.Conf.CREEP 7, JSME, No.01, Vol.201, Ed. Y.Asada, 2001, p.123.

[3] Dogan, B., Int. J.of Pressure Vessels and Piping, 80, 2003, pp.149-156.

[4] Dogan, B., and Ainsworth, R.A., ASME Conf. PVP2003-2032, Vol.463, 2003, pp.105-111.

[5] British Standard BS7910, "Guidance on methods for assessing the acceptability of flaws in metallic structures", British Standards Institution, 2000.

[6] ASME Section III, Rules for construction of nuclear power plant components, Division 1, Sub-section NH, Class 1 components in elevated temperature service, ASME, 1995.

[7] R5, "Assessment procedure for the high temperature response of structures", Ed. Goodall I.W., British Energy-UK, Issue 2, 1998.

[8] A16, "Guide for Leak Before Break Analysis and Defect Assessment" RCC-MR, Appendix A16, Edition 2002, AFCEN No: 94-2002.

[9] Drubay B., Moulin D., Faidy C., Poette C. and Bhandari S., Defect assessment procedure: A French approach, ASME PVP, Vol. 266, 1993, pp. 113-118.

[10] Jaske, C. E., Materials data needs for fatigue design of pressure vessel systems, in STP 770, Low cycle Fatigue and Life Prediction, Ed. C. Amzallag et al., ASTM, Philadelphia, 1982, pp. 600-611.

[11] ASTM E1457-00, "Standard test method for measurement of creep crack growth rates in metals", ASTM 03.01, Philadelphia: ASTM 2000, PA 19103, USA.

[12] Saxena A. and Liaw P.K., Remaining Life Assessment of Boiler Pressure Parts-Crack Growth Studie, EPRI CS 4688, Electric Power Research Institute, Palo Alto, CA, 1986.

[13] Dogan B., Saxena A. and Schwalbe K.-H. Materials at High Temperatures, May 1992, Vol.10, No.2, pp.138-143.

[14] Dogan B., Petrovski B. and Schwalbe K.-H. Int. Conf. "Integrity of High Temperature Welds" Forte Posthouse, Nottingham, U.K., 3-4. 11.1998.

[15] Riedel H. and Detampel V. Int. J. of Fracture, 1988; Vol.36, pp.275-289.

[16] Hawk D.E. and Bassani J.L., J. Mechanics and Physics of Solids, Vol.34, No.3, 1986, pp.191-212.

[17] Dean, D.W. and Hooton, D.G., A Review of Creep Toughness Data for Austenitic Type 316 Steels, BEGL Report E/REP/GEN/0024/00, 2003.

[18] Ainsworth, R.A, Hooton, D.G.and Green, D., Failure Assessment Diagrams for High Temperature Defect Assessment, Vol.62, 1999, pp.95-109.

[19] Riedel, H. and Rice, J.R., ASTM STP 700, 1980, p.112.

[20] Holdsworth, S.R., Materials at High Temperatures, Vol.10, No.2, May 1992, pp.127-137.

[21] Dogan, B., Petrovski, B. and Ceyhan, U., Proc. Int. Conf. BALTICA VI, VTT Symposium 234, Vol.2, Eds. J.Veivo and P.Auerkari, Espoo, Finland, pp.595-607.

[22] Ainsworth, R. A. and Budden, P. J., Design and assessment of components subjected to creep, J. Strain Anal., Vol.29, 1994, pp.201-208.

[23] R6, Assessment of integrity of structures containing defects, Procedure R6, Revision 3, British Energy, Gloucester, UK, 1997.

[24] Ainsworth, R.A., Fatigue Fract. Engng. Mater. Struct., 16, 1993. pp.1091-1108.

[25] F Müller, T Gengenbach, A Klenk, ECCC CCI (WG 1.2) Volume 3 (Part IV), Draft 3, 30/06/2003

[26] Pique, R., Bensussan, P. and Pineau, A., Proc. MECAMAT, Int. Seminar on High Temperature Fracture Mechanisms and Mechanics, Dourdan, France, 1987.

[27] Dogan, B. Petrovski, B., Ceyhan, U., Proc. of ECCC Int. Conf. on Creep and Fracture in High Temperature Components – Design and Life Assessment Issues, Eds. I.A. Shibli, S.R. Holdsworth, G. Merckling, London, UK, 2005, pp.724-743.

[28] Davies, C.M., O'Dowd, N.P.,Dean, D.W, Nikbin, K.M. and Ainsworth, R.A., Int.J.Pressure Vessels and Piping, 80, 2003, pp.541-551.